Hindawi
Advances in Condensed Matter Physics
Volume 2019, Article ID 8767640, 8 pages
https://doi.org/10.1155/2019/8767640

Review Article

A Simplified Scaling Law of Cell-Dendrite Transition in Directional Solidification

Yaochan Zhu,[1,2] **Hua Qiu**,[1] **Zhijun Wang**,[2] **and Eckart Schnack**[3]

[1]*Xi'an Aeronautical Polytechnic Institute, Xi'an 710089, China*
[2]*State Key Laboratory of Solidification Processing, Northwestern Polytechnical University, Xi'an, China*
[3]*Karlsruhe Institute of Technology, Karlsruhe 76131, Germany*

Correspondence should be addressed to Yaochan Zhu; zhuyaocan1978@hotmail.com

Received 11 February 2019; Revised 11 May 2019; Accepted 21 May 2019; Published 2 June 2019

Academic Editor: Kiyokazu Yasuda

To describe the cell-dendrite transition (CDT) during directional solidification, a new simplified scaling law is proposed and verified by quantitative phase field simulations. This scaling law bears clear physical foundation with consideration of the overall effects of primary spacing, pulling velocity, and thermal gradient on the onset of sidebranches. The analysis results show that the exponent parameters in this simplified scaling law vary within different systems, which mediates the discrepancy of exponent parameters in previous experiments. The scaling law also presents an explanation for the destabilizing mechanism of thermal gradient in sidebranching dynamics.

1. Introduction

As one of the typical problems of pattern formation, solidification microstructures are interesting for both scientific and technologic reasons [1–3]. Though remarkable progress in the study of microstructure evolution during solidification has been made, the mechanism of sidebranching dynamics is still unsatisfactorily understood [4–6]. During directional solidification, the onset of sidebranches means the occurrence of cell-dendrite transition (CDT). Over past few years, the identification of CDT has been widely performed experimentally [7–11], which showed that cell and dendrite coexist over a large range of control parameters. Given pulling velocity and thermal gradient, small primary spacing corresponds to cellular morphology in CDT region, while large primary spacing corresponds to dendrite. Accordingly, CDT significantly depends on the primary cellular/dendritic spacing, and a critical primary spacing λ_{1CD} corresponding to CDT should exist. In terms of the correlation between λ_{1CD} and control parameters, researchers have put much effort all along on finding the criteria of CDT by considering the spacing, pulling velocity V, and thermal gradient G. Based on abundant experiments [7–10], an empirical scaling law with the form of $\lambda_{1CD} \propto V^{\alpha} G^{\beta}$ has been summarized to describe the critical primary spacing λ_{1CD} in which α and β are exponent parameters.

Although the form of scaling law has been proposed, some controversies still exist. On one hand, the values of the exponent α and β are inconsistent in different experiments. $\alpha = -1/2$ and $\beta = -1/8$ were found in Gerogelin et al.'s experiments [7] and $\alpha = \beta = -1/3$ in Trivedi et al.'s experiments [8, 9]. On the other hand, this empirical scaling law was based on the data fitting without further physical foundation. Researchers have tried to expound the intrinsic physical foundation of the scaling law. In Trivedi et al.'s work [8], the critical primary spacing λ_{1CD} was given by the geometrical meaning of three characteristic lengths: solutal diffusion length l_D, thermal length l_T, and capillary length d_0. Gerogelin et al. [7] also presented a self-similar asymptotic regime about l_T/l_D, λ_{1CD}/d_0, and l_T/d_0 based on their experimental data. However, these analyses only focused on the assembly of characteristic lengths, not referring to the sidebranching dynamics, which characterizes the CDT. The exponent parameters selection and the physical foundation in the scaling law of CDT are still unclear and need further exploration.

The crossover of CDT is usually defined by the occurring of sidebranches. Accordingly, sidebranching should be one

of the typical characteristics in CDT, and the connections between the scaling law and sidebranching dynamics should exist. However, previous scaling law did not take sidebranching dynamics into account. Therefore, it should be more reasonable to characterize CDT by the onset of sidebranching instability. Furthermore, the empirical scaling law indicates that, beyond CDT, increasing the thermal gradient G will enhance the sidebranching dynamics. This destabilizing effect of thermal gradient G on the sidebranching dynamics has been observed in [7–10]. Noise amplification theory failed in describing the effect of thermal gradient G on sidebranching dynamics [7]. Therefore, to acquire a deep understanding of CDT and sidebranching, it is essential to propose more reasonable physical explanations on the scaling law and the destabilizing mechanism.

Although sidebranching dynamics has received considerable attentions in free dendritic growth [1, 4–6], only some basic understanding about the sidebranching dynamics has been obtained in directional solidification [7, 10–15]. Gerogelin et al [7] presented a model to describe the sidebranching dynamics, in which the noise amplitude at the cellular tip was controlled by the feedback of sidebranches. However, it is difficult to determine the growth factor in their model. On the other hand, experimental results and phase field simulations indicated that the diffusion instability of dendritic trunk is the most possible reason for sidebranching dynamics [14–16] and revealed that the initial sidebranching spacing only depends on the pulling velocity, but the sidebranch amplitude is determined not only by pulling velocity V but also by the primary spacing and the thermal gradient G. With consideration of the overall effects of primary spacing, pulling velocity V, and thermal gradient G on the onset of sidebranches, the scaling law of CDT may gain more physical foundation.

In this article, firstly, we briefly review the factors in determining the onset of sidebranches from previous experiments and quantitative phase field simulations. Then a new scaling law of CDT is proposed based on the sidebranching dynamics and the physical foundation of this new scaling law is presented. The effects of pulling velocity and thermal gradient on CDT will be analyzed according to this new scaling law. Finally, the quantitative phase field simulations will be used to testify this proposed scaling law.

2. Factors Determining Sidebranches during Directional Solidification

It has been widely accepted that the primary spacing λ_1, pulling velocity V, and thermal gradient G play an important role in determining the sidebranches dynamics. The effects of λ_1, V, and G on the dendritic growth have also been well studied. Here the related results and how the sidebranching dynamics is affected by the controlled parameters are recalled briefly.

Primary spacing λ_1 affects the sidebranch dynamics significantly. In experiments, the microstructures near the CDT show dendritic array with large spacing and cellular array with small spacing [7–10]. Quantitative phase field simulations revealed the intrinsic reason [15, 17] that the smaller spacing suppresses the sidebranch growth due to the strong interdendritic solutal interaction. However, after the appearance of sidebranch, the location of first sidebranch and the initial sidebranch spacing are almost independent of primary spacing. Therefore, the primary spacing only influences the amplitude of the sidebranch but does not change the initial sidebranch spacing. Accordingly, the primary spacing only supplies spacing for sidebranch growth.

Pulling velocity V is an important control parameter during directional solidification. According to experimental investigations and simulation, the initial sidebranch spacing λ_2 has a scaling law with the pulling velocity $\lambda_2 \infty V^{\alpha}$ [7, 14, 15, 18]. Dendrite trunk also depends on the pulling velocity greatly. The width of dendrite trunk decreases as pulling velocity increases. Within the same primary spacing, the decrease of pulling velocity enlarges the diffusion length, which enhances the interdendritic interaction and suppresses the sidebranch growth. As aforementioned, the interdendritic interaction does not change the initial sidebranch spacing. Therefore, the variation of initial sidebranch spacing is mainly attributed to the variation of pulling velocity. In previous investigations, the variation of initial sidebranch spacing λ_2 with pulling velocity satisfies $\lambda_2 \infty V^{-0.59}$ [7, 14, 18].

The role of thermal gradient G in sidebranch growth is a little bit complex. Previous investigation on the cell-dendrite transition indicated that positive thermal gradient promotes the generation of sidebranch [7], but the initial sidebranch spacing λ_2 was independent of thermal gradient G [14]. It is attributed to the remarkable interdendritic solutal interaction near CDT, where the thermal gradient G significantly affects the mush zone in directional solidification. However, the details on the thermal gradient effects are still absent and some confusion still exists. For example, the effects of thermal gradient on dendritic morphologies are relatively weaker for dendritic array growth, where the sidebranch amplitude is almost independent of thermal gradient [15].

3. Scaling Law of CDT from Sidebranching

From the above review, we can found that previous investigations have presented lots of details about sidebranching dynamics during directional solidification However, the intrinsic sidebranching mechanism during directional solidification is still not fully revealed. Compared with free growth, the interdendritic interaction will suppress the sidebranch growth, so the interdendrite interaction plays an important role in determining the sidebranches. It is still difficult to reveal CDT by directly deriving the sidebranching amplitude evolution from the basic diffusion equation and interface condition.

Here we focus on the interdendritic solutal interaction to reveal the CDT and derive the scaling law of CDT in the following. Sketch of the dendrite with sidebranches and definition of parameters during the derivations are shown in Figure 1, where ρ_{tip} is the dendritic tip radius, z_{tip} is the tip position along z-axis, λ_1 is primary spacing, λ_2 is the

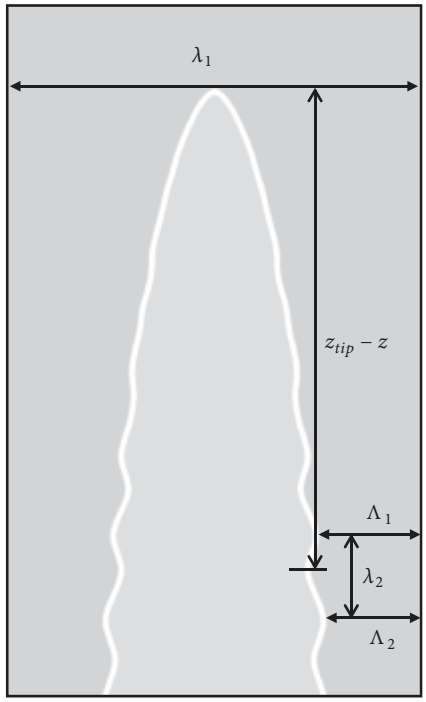

Figure 1: Sketch of sidebranches and parameters definition in the derivation of scaling law, where λ_1 is primary spacing, λ_2 is the sidebranch spacing, Λ_1 and Λ_2 are groove width, and z_{tip} is the tip position along z-axis.

sidebranch spacing, and Λ_1 and Λ_2 are groove width. The parameter definitions are as follows: solutal diffusion length $l_D = D/V$, thermal length $l_T = \Delta T_0/G$, and capillary length $d_0 = \Gamma/\Delta T_0$, where D is the liquid solutal diffusion coefficient, $\Delta T_0 = mC_0(k\text{-}1)/k$, Γ is the Gibbs-Thomson coefficient [3], C_0 is the initial alloys composition, m is the liquid slope, and k is the equilibrium solute-partition coefficient. In the interdendrite region, we define the groove width 2Λ and lateral diffusion length $l_{LD} = D/V_L$, where V_L is the lateral interface velocity.

Here, the CDT is characterized by the appearance of sidebranches. Sidebranches firstly appear near the dendritic tip and then are amplified in the groove by the lateral growth of dendritic trunk. Two assumptions are adopted in the derivation: (1) the occurrence of CDT corresponds with the visibility of sidebranches; (2) the intrinsic conditions for sidebranching are based on the fact that the lateral diffusion accelerates the lateral instability, while the groove width blocks the lateral instability. According to assumption (1), the ratio of the sidebranch amplitude A and the sidebranch wavelength λ_2 can be adopted to characterize the CDT. According to assumption (2), CDT is determined by the competition between the lateral diffusion length l_{LD} and the groove width 2Λ. Both l_{LD} and 2Λ have the length dimension, so the groove instability can be assumed to be proportional to the groove width 2Λ and inversely proportional to the lateral diffusion length l_{LD}. Therefore, the two dimensionless characteristics A/λ_2 and Λ/l_{LD} can be the representative of dimensionless characterization and driving force of sidebranching dynamics, respectively. For smaller sidebranch amplitude, A/λ_2 is a function of Λ/l_{LD}:

$$\frac{A}{\lambda_2} = f\left(\frac{\Lambda}{l_{LD}}\right) \tag{1}$$

Near CDT, the lateral diffusion length is very large and the groove width is small, which results in that the Λ/l_{LD} approaches zero. With Taylor expansion of $A/\lambda_2 \approx f(0) + f'(0)\Lambda/l_{LD} + o((\Lambda/l_{LD})^2)$, we can assume that the relationship between the driving force and the characterization of the sidebranch is linear near CDT, where both A/λ_2 and Λ/l_{LD} are very small. Then the function in (1) can be approximated by a linear function: $A/\lambda_2 \sim \Lambda/l_{LD}$ or $A \sim \lambda_2\Lambda/l_{LD}$. If we define certain finite amplitude A as the representation of sidebranches appearance, then this finite amplitude A leads to a constant $\lambda_2\Lambda/l_{LD}$ at CDT for different pulling velocities and thermal gradients.

According to the asymptotic analysis of dendrite growth in directional solidification by Spencer and Huppert [19], in the region of $\rho_{tip} \ll z_{tip} - z \ll l_T$ as shown in Figure 1, we have

$$\Lambda = \frac{\lambda_1\left(1 - a - \sqrt{\left(z_{tip} - z\right)/l_T}\right)}{2} \tag{2}$$

where a is a modified parameter to represent the dendritic trunk width in the groove. Then, within a period of sidebranches, the lateral interface velocity V_L and the lateral diffusion length l_{LD} can be represented as

$$V_L = \left(\Lambda_1 - \Lambda_2\right)\left(\frac{\lambda_2}{V}\right) \tag{3}$$

$$l_{LD} \propto \frac{4l_D\sqrt{l_T\left(z_{tip} - z\right)}}{\lambda_1} \tag{4}$$

In experiments, the visible amplitude is most likely to appear at $z = z_{tip}\text{-}n\lambda_2$, where n is a constant [7, 8]. According to (1)–(4), a new simplified scaling law of CDT can be described as

$$\lambda_{1CD} \sim \lambda_2^{-1/4} l_D^{1/2} l_T^{1/4}\left(1 - a - \left(n\lambda_2\right)^{1/2} l_T^{-1/2}\right)^{-1/2} \tag{5}$$

In formula (5), sidebranch spacing λ_2 and solutal diffusion length $l_D = D/V$ are related to the pulling velocity V while thermal length $l_T = \Delta T_0/G$ is related to the thermal gradient G. The first three terms on the right side of formula (5) are directly connected to the exponent parameters in the scaling law of $\lambda_{1CD} \infty V^{\alpha} G^{\beta}$, while the contribution of the last term $(1 - \alpha - (n\lambda_2)^{1/2} l_T^{-1/2})^{-1/2}$ to the exponent parameters depends on λ_2/l_T. According to this new scaling law, the effects of pulling velocity V and thermal gradient G on the CDT can be well addressed.

To validate this new scaling law, the data in [12] is adopted as a paradigm for further analysis. To describe the effect of thermal length l_T more conveniently, we define

$$f\left(l_T\right) = l_T^{1/4}\left(1 - a - \left(n\lambda_2\right)^{1/2} l_T^{-1/2}\right)^{-1/2} \tag{6}$$

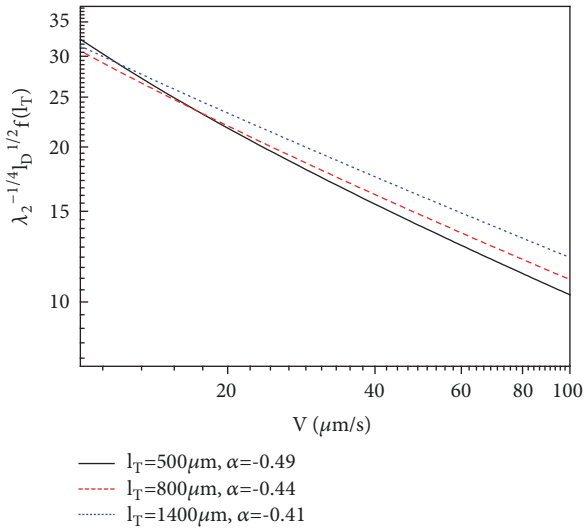

FIGURE 2: The scaling law between the critical primary spacing and the pulling velocity with different thermal lengths in the cell-dendrite transition, described by formula (5), where $\lambda_2 \approx 350V^{-0.6}$, a=0.1, and n=2.

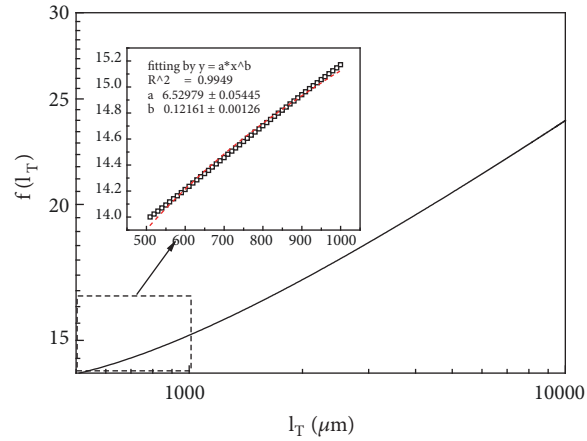

FIGURE 3: The effect of the thermal length on the scaling law of formula (5). The inset presents the local region with power law fitting. The corresponding parameters are $\lambda_2 \approx 350V^{-0.6}$ with V=50 $\mu m/s$, a=0.1, and n=2.

According to the data in [12], the relationship between sidebranch spacing λ_2 and pulling velocity V is $\lambda_2 \approx 350V^{-0.6}$, the thermal length l_T is about 500~1400 μm, and the parameters of a and n in (6) are 0.1 and 2, respectively.

In the above new scaling law described by formula (5), the exponent parameter α for pulling velocity V is not constant but is related to the thermal gradient G. Figure 2 shows the effect of l_T on the exponent parameter α. When l_T increases from 500 μm to 1400 μm, α increases from -0.49 to -0.41 correspondingly. It shows that, within the range of l_T = 500~1400 μm, the value of α consists with the scaling law proposed by Gerogelin et al. ($\alpha = -1/2$) [7], where $\alpha = -0.46$ in uniform cellular/dendritic array. When λ_2/l_T is small enough, we have $\lambda_{1CD} \sim \lambda_2^{-1/4} l_D^{1/2} l_T^{1/4} \sim V^{-0.35}$; then α will be -0.35, which agrees with the result of Trivedi et al.'s experiments [8, 9].

As to the exponent parameter β for thermal gradient G in the scaling law, Figure 3 shows the variation of $f(l_T)$ with l_T. When l_T is small, the effect of the term $(1 - a - (n\lambda_2)^{1/2} l_T^{-1/2})^{-1/2}$ cannot be overlooked. As shown in the inset, the power function fitting gives the exponent β as –0.122, which is consistent with the fitting results in Gerogelin et al.'s experiments ($\beta = -1/8$) [7]. As the thermal gradient G decreases, l_T increases and the variation of term $(1 - a - (n\lambda_2)^{1/2} l_T^{-1/2})^{-1/2}$ makes the exponent parameter β increase. As shown in Figure 3, large l_T ensures $\beta = -1/4$ ($\lambda_{1CD} \sim \lambda_2^{-1/4} l_D^{1/2} l_T^{1/4} \sim G^{-1/4}$). Therefore, for a small thermal gradient corresponding to large l_T, the exponent parameter of the thermal gradient in the scaling law is very close to Trivedi et al.'s results [8, 9].

The form of this scaling law can return back to the empirical one and reconciles the difference of the exponent parameters in previous experiments. Analysis on the exponent parameters in the scaling law of $\lambda_{1CD} \infty V^{\alpha} G^{\beta}$ indicates the variation of exponents α and β with different solidification systems. When $\lambda_2/l_T \longrightarrow 0$, $\lambda_{1CD} \sim \lambda_2^{-1/4} l_D^{1/2} l_T^{1/4} \sim V^{-0.35} G^{-1/4}$, that is, α=-0.35 and β=-0.25, which is close to Trivedi et al.'s experimental results [8, 9]. Previous experiment also mentioned that the change of thermal gradient G influences the exponent parameters. Teng et al. [9] pointed out that the increase of thermal gradient G induces a larger systematic deviation from $\alpha = \beta = -1/3$. Similarly, in Gerogelin et al.'s experiments [7], the thermal gradient G was relatively large and $\alpha = -0.5$ and $\beta = -1/8$. This agrees with the analysis presented here, which shows that the exponent parameters vary with thermal gradient G. For a large thermal gradient G, the exponent parameter may be selected as $\alpha = -0.45$ and $\beta = -0.122$. Accordingly, the power law presented here could settle the argument in previous experiments about the discrepancy of exponent parameters.

As to the destabilizing effect of thermal gradient G on the sidebranching dynamics, it also can be explained according to this new scaling law. The sidebranching instability is determined by the competition between lateral diffusion length l_{LD} and the groove width 2Λ. Both of l_{LD} and Λ decrease with the increase of thermal gradient G. Small diffusion length implies the enhanced diffusion instability, while small groove width is helpful to stabilize the cell. However, from (2), (3), and (4), we can get $\Lambda/l_{LD} \sim (1 - a)/\sqrt{l_T(z_{tip} - z)} - 1$, so Λ/l_{LD} decreases with the thermal length l_T; that is, Λ/l_{LD} increases with the thermal gradient G. This indicates that the effect of thermal gradient G on the lateral diffusion length l_{LD} predominates. The destabilizing effect of thermal gradient G comes from the decrease of lateral diffusion length l_{LD}, which is similar to the destabilizing effect of increasing pulling velocity V in planar instability [1, 20, 21]. So the lateral diffusion length l_{LD} bridges the thermal gradient G and the sidebranching instability, which can be used to explain the destabilizing nature of thermal gradient.

The scaling law here is related to three parameters, the sidebranch spacing, the diffusion length, and the thermal

length, which are related to the undercooling and thermal gradient, respectively. In experiments, all these parameters vary in different systems with different parameters. Accordingly, the validity of the scaling law can be well checked with designed experiments. In this research, the new scaling law will be validated by a benchmark from quantitative phase field simulation instead.

Note that the noise effects on the sidebranching dynamics in dendrite growth have been a controversial issue for many years [22]. However, there is an agreement that the presence of stochastic noise will not affect the frequency of sidebranching, while the value of the amplitude is a function of noise intensity level. Just as predicted by [23], the transition of cellular to dendrite growth may be modified by the noise intensity level. In the derivation of the scaling law, the sidebranching amplitude is considered as a function of three length scales that are independent of the noise. Therefore, the noise may affect the transition points, but the scaling law between these lengths still exists. At an adequate noise level similar to that in the experiment, the scaling law is valid.

4. Validation of the Scaling Law by Phase Field Simulation

The development of phase field method makes it possible to quantitatively investigate microstructure evolution in solidification [18] and the quantitative phase field simulation has been widely used to investigate the sidebranching dynamics in crystal growth [6, 15, 16] and the primary spacing selection mechanism in directional solidification [17, 24–26]. To further validate the scaling law, the quantitative phase field method [18] is employed. For the directional solidification simulation by (7) and (8), assume one-sided diffusion and frozen temperature approximation, in which $T = T_C + Gz$ and T_C is the temperature at the cooling end and G is the thermal gradient along z-axis. The dynamic evolution equations of phase field model in the moving frame with pulling velocity V are

$$\begin{aligned}\tau_0 &\left(1-(1-k)\frac{z+\left(mc_\infty/k\right)/G}{l_T}\right)\left(\partial_t\phi - V\partial_z\phi\right)\\ &= \nabla\left(W(\theta)^2\nabla\phi\right) - \partial_x\left[W(\theta)W'(\theta)\partial_y\phi\right]\\ &+ \partial_y\left[W(\theta)W'(\theta)\partial_x\phi\right] + \phi - \phi^3 + \lambda\left(1-\phi^2\right)^2\left(U\right.\\ &\left.+\frac{z+\left(mc_\infty/k\right)/G}{l_T}\right)\end{aligned} \tag{7}$$

$$\begin{aligned}\partial_t c - V\partial_z c = \nabla\cdot\Bigg[&D_L\frac{1-\phi}{1+k-(1-k)\phi}\nabla c\\ &+\left(D_L\frac{1-\phi}{1+k-(1-k)\phi}+\frac{W_0}{\sqrt{2}}\frac{\left(\partial_t\phi - V\partial_z\phi\right)}{|\nabla\phi|}\right)\\ &\cdot\frac{c(1-k)}{1+k-(1-k)\phi}\nabla\phi\Bigg]\end{aligned} \tag{8}$$

with

$$W(\theta) = W_0\left(1+\gamma_4\cos 4\theta\right) \tag{9}$$

$$U = \frac{\left(\left(2kc/c_\infty\right)/\left(1+k-(1-k)\phi\right)-1\right)}{(1-k)} \tag{10}$$

$$l_T = \frac{|m|\,c_\infty(1-k)}{(kG)} \tag{11}$$

where W_0 are the parameters of the interface thickness, τ_0 is the relaxation time for phase field model, and λ is the coupling constant, which are related to physical quantities by $d_0 = a_1 W_0/\lambda$ and $\tau_0 = a_2\lambda W_0^2/D$; γ_4 is the anisotropic intensity of the surface tension, θ is the angle between the normal vector of the interface and the preferred orientation, m is the liquidus slope, k is the partition coefficient, and c_∞ is the concentration in the far away field. Here $d_0 = \Gamma/(mc_\infty(1\text{-}k)/k)$, a_1=0.8839, and a_2=0.6267, and Γ is the Gibbs-Thomson coefficient.

The transparent alloy SCN-0.43wt%C152 is adopted, which has been widely used to investigate the evolution of dendritic pattern [27]. The chemical diffusion coefficient of the liquid phase is $D \approx 0.45\times10^{-9}$ m^2/s, partition coefficient k=0.05, Gibbs-Thomson coefficient $\Gamma = 6.48\times10^{-8}$ K/m, and the slope of liquidus line m=-542 K/mol. The surface tension anisotropy intensity is assumed as γ_4=0.005.

This quantitative phase field simulation on dendritic growth with the presented parameters has been widely performed in our previous investigations [15, 17]. The phase field simulation on the sidebranching indicates that $\lambda_2 = 150V^{-0.59}$ and the parameters a and n in (6) are about 0.4 and 5, respectively. Then the exponents in the new proposed scaling law for the simulation system are $\alpha = -0.35$ and $\beta = -0.21$ according to formula (5), which are different from $\alpha = \beta = -1/3$ [8, 9] and $\alpha = -1/2$ and $\beta = -1/8$ [7]. These three different groups of exponents will be quantitatively examined according to the phase field simulation results.

Here, a benchmark is designed to directly compare the exponents in different scaling laws. The exponents are usually obtained by fitting plenty of simulation or experiment results with different control parameters. However, heavy workload and artificial judgment on the onset of sidebranching are required by this method. In a different way, we design a benchmark instead of finding the exponents in the simulation system as follows. The steady state of interface morphology in specific primary spacing with onset of sidebranching is firstly presented, where the thermal gradient G_0 and pulling velocity V_0 as well as the morphology will be the references. Then, the critical pulling velocity for the CDT can be extrapolated from different scaling laws along with the variation of thermal gradient G in the fixed primary spacing. The solid/liquid morphologies corresponding to the different critical velocities are obtained by phase field simulation. Finally, by comparing the simulation results with the reference morphology, the scaling law with different exponents is evaluated. Here G_0=20.2 K/cm and V_0=20 $\mu m/s$ are chosen as the referential control parameters. The critical primary spacing for CDT is λ_1=160 μm and the referential morphology is shown in Figure 4(a). With λ_1=160

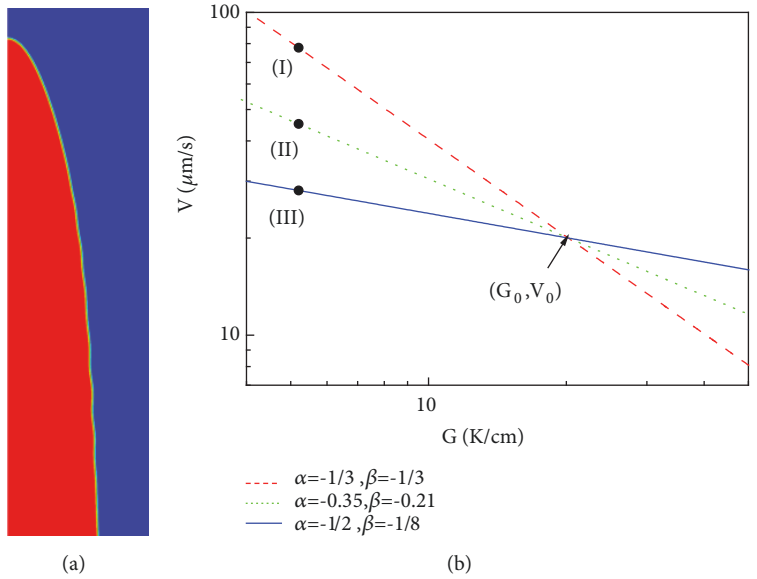

FIGURE 4: The critical microstructure of cell-dendritic transition at the benchmark (a) and the criteria of cell-dendrite transition according to the different power laws based on the benchmark (b).

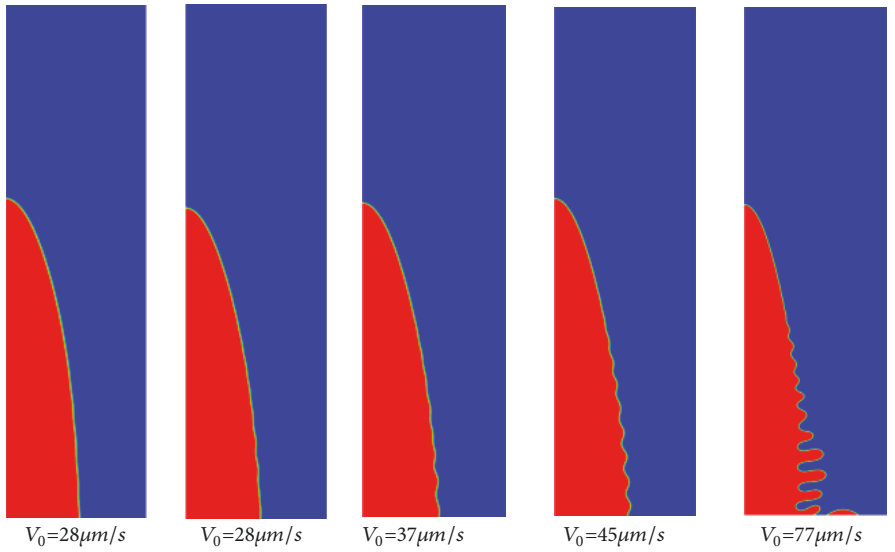

FIGURE 5: The cellular/dendritic morphologies with different pulling velocities when G=5.2 K/cm.

μm and G_0=5.2 K/cm, the different critical pulling velocities for CDT are V_{I}=77 $\mu m/s$, V_{II}=45 $\mu m/s$, and V_{III}=28 $\mu m/s$, respectively, for three groups of exponent parameters (-1/3, -1/3), (-0.35, -0.21), and (-1/2, -1/8), as shown by the dot in Figure 4(b).

Figure 5 presents the cellular/dendrite morphologies for different pulling velocities with λ_1=160 μm and G_0=5.2 K/cm. Compared with the referential morphology in Figure 4(a), the critical pulling velocity is around 35 $\mu m/s$. The pulling velocity 77 $\mu m/s$ predicted by (-1/3, -1/3) is obviously larger than the critical pulling velocity for CDT, while the pulling velocity 28 $\mu m/s$ predicted by (-1/2, -1/8) is close to the critical pulling velocity but with cellular morphology. The pulling velocity 45 $\mu m/s$ from the new proposed scaling is also close to the critical pulling velocity of CDT.

The critical pulling velocity of CDT can be further found within higher accuracy. In the simplified form of the new proposed scaling law (formula (5)), the contribution of the term λ_2/l_T on the critical pulling velocity in (6) is overlooked. Here, by submitting λ_2=150$V^{-0.59}$ into (6), the effect of the term λ_2/l_T can be revealed. Considering the overall effects of thermal gradient G and pulling velocity V, the variation of the left-hand side of formula (5) with pulling velocity for two different thermal gradients is presented in Figure 6. It shows that the exponent α is near -0.35 with small thermal gradient G. However, α deviates from -0.35 gradually as the

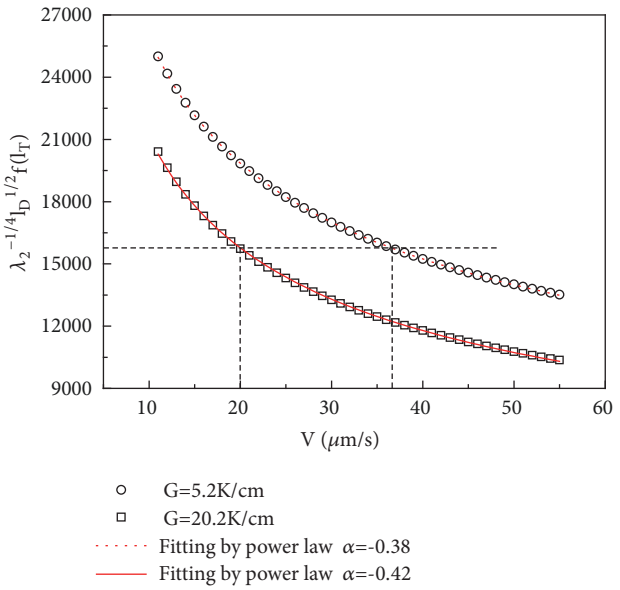

FIGURE 6: The variation of the value of right-hand side in (5) with pulling velocity for different thermal gradients.

thermal gradient G increases, which means that the influence of pulling velocity V on λ_2/l_T has significant impact on $f(l_T)$ with relatively small l_T. Considering the contribution of pulling velocity V on $f(l_T)$, Figure 6 gives the critical pulling velocity of CDT as $37\mu m/s$ when λ_1=160 μm and G_0=5.2 K/cm in the simulation system. The interface morphology for 37 $\mu m/s$ is very close to the reference morphology in the benchmark.

5. Results and Discussion

To summarize, a simplified scaling law of CDT during directional solidification is derived with considering the sidebranching dynamics. The exponent parameters corresponding to the pulling velocity and thermal gradient in the new scaling law are discussed. The analysis shows that the exponent parameters in the scaling law vary with different solidification systems and reconcile the discrepancy in previous experimental results. The form of this scaling law can return back to the empirical one and reconciles the difference of the exponent parameters in previous experiments. The destabilizing mechanism of thermal gradient in the sidebranching dynamics can be revealed by lateral diffusion length. The new scaling law is also validated by a benchmark from quantitative phase field simulation. The appropriate experimental verification of the scaling law can be similar to that done by Teng et al [9]. With the apparatus, one can use different systems and parameters to check the cellular-to-dendrite transition.

Furthermore, the proposed scaling law is more than the conciliation of the controversy in previous experiments. On one hand, compared with previous scaling law, the new scaling law is with more physical foundation related to the sidebranching dynamics. On the other hand, it indicates that the thermal gradient and pulling velocity are coupled together in describing the CDT within a large range parameter space. Only in local parameter space, the scaling law of CDT has a simple form consisted with previous experimental results where the thermal gradient and pulling velocity are decoupled. Therefore, the proposed scaling law is with more precision in predicting CDT in a large range parameter space compared with previous investigations.

Conflicts of Interest

The authors declare that they have no conflicts of interest.

Acknowledgments

The work was supported by the fund of the State Key Laboratory of Solidification Processing in NWPU (Grant no. SKLSP201725).

References

[1] J. S. Langer, "Instabilities and pattern formation in crystal growth," *Reviews of Modern Physics*, vol. 52, no. 1, pp. 1–28, 1980.

[2] M. C. Cross and P. C. Hohenberg, "Pattern formation outside of equilibrium," *Reviews of Modern Physics*, vol. 65, no. 3, pp. 851–1112, 1993.

[3] W. J. Boettinger, S. R. Coriell, A. L. Greer et al., "Solidification microstructures: recent developments, future directions," *Acta Materialia*, vol. 48, no. 1, pp. 43–70, 2000.

[4] A. Karma and W.-J. Rappel, "Phase-field model of dendritic sidebranching with thermal noise," *Physical Review E: Statistical Physics, Plasmas, Fluids, and Related Interdisciplinary Topics*, vol. 60, no. 4, pp. 3614–3625, 1999.

[5] M. E. Glicksman, J. S. Lowengrub, S. W. Li et al., "A deterministic mechanism for dendritic solidification kinetics," *The Journal of the Minerals Metals & Materials Society*, vol. 59, no. 8, pp. 27–34, 2007.

[6] Z. Wang, J. Wang, and G. Yang, "Phase-field investigation of effects of surface-tension anisotropy on deterministic sidebranching in solutal dendritic growth," *Physical Review E: Statistical, Nonlinear, and Soft Matter Physics*, vol. 78, no. 4, Article ID 042601, 2008.

[7] M. Georgelin and A. Pocheau, "Onset of sidebranching in directional solidification," *Physical Review E: Statistical Physics, Plasmas, Fluids, and Related Interdisciplinary Topics*, vol. 57, no. 3, pp. 3189–3203, 1998.

[8] R. Trivedi, Y. Shen, and S. Liu, "Cellular-to-dendritic transition during the directional solidification of binary alloys," *Metallurgical and Materials Transactions A: Physical Metallurgy and Materials Science*, vol. 34, no. 2, pp. 395–401, 2003.

[9] J. Teng, S. Liu, and R. Trivedi, "Onset of sidewise instability and cell-dendrite transition in directional solidification," *Acta Materialia*, vol. 57, no. 12, pp. 3497–3508, 2009.

[10] G. L. Ding, *On primary dendritic spacing during unidirectional solidification [PhD thesis]*, Northwestern Polytechnical University, Xi'an, China, 1997.

[11] E. Acer, E. Çadırlı, H. Erol, H. Kaya, and M. Gündüz, "Effects of growth rates and compositions on dendrite arm spacings in directionally solidified Al-Zn alloys," *Metallurgical and Materials Transactions A: Physical Metallurgy and Materials Science*, vol. 48, no. 12, pp. 5911–5923, 2017.

[12] A. Pocheau, S. Bodea, and M. Georgelin, "Self-organized dendritic sidebranching in directional solidification: sidebranch coherence within uncorrelated bursts," *Physical Review E: Statistical, Nonlinear, and Soft Matter Physics*, vol. 80, no. 3, Article ID 031601, 2009.

[13] J. S. Kirkaldy, L. X. Liu, and A. Kroupa, "Thin film forced velocity cells and cellular dendrites-II. Analysis of data," *Acta Metallurgica et Materialia*, vol. 43, no. 8, pp. 2905–2915, 1995.

[14] K. Somboonsuk, J. T. Mason, and R. Trivedi, "Interdendritic spacing: part I. Experimental studies," *Metallurgical Transactions. A, Physical Metallurgy and Materials Science*, vol. 15, no. 6, pp. 967–975, 1984.

[15] Z. J. Wang, J. C. Wang, and G. C. Yang, "Phase field investigation on the selection of initial sidebranch spacing in directional solidification," *IOP Conference Series: Materials Science and Engineering*, vol. 27, no. 1, p. 012009, 2012.

[16] B. Echebarria, A. Karma, and S. Gurevich, "Onset of sidebranching in directional solidification," *Physical Review E: Statistical, Nonlinear, and Soft Matter Physics*, vol. 81, no. 2, Article ID 021608, 2010.

[17] Z. Wang, J. Li, J. Wang, and Y. Zhou, "Phase field modeling the selection mechanism of primary dendritic spacing in directional solidification," *Acta Materialia*, vol. 60, no. 5, pp. 1957–1964, 2012.

[18] B. Echebarria, R. Folch, A. Karma, and M. Plapp, "Quantitative phase-field model of alloy solidification," *Physical Review E: Statistical, Nonlinear, and Soft Matter Physics*, vol. 70, no. 6, Article ID 061604, 2004.

[19] B. J. Spencer and H. E. Huppert, "Relationship between dendrite tip characteristics and dendrite spacings in alloy directional solidification," *Journal of Crystal Growth*, vol. 200, no. 1-2, pp. 287–296, 1999.

[20] Z. Wang, J. Wang, and G. Yang, "Onset of initial planar instability with surface-tension anisotropy during directional solidification," *Physical Review E: Statistical, Nonlinear, and Soft Matter Physics*, vol. 80, no. 5, Article ID 052603, 2009.

[21] Z. Wang, J. Wang, and G. Yang, "Fourier synthesis predicting onset of the initial instability during directional solidification," *Applied Physics Letters*, vol. 94, no. 6, p. 061920, 2009.

[22] J. J. Xu, *Interfacial Wave Theory of Pattern Formation in Solidification: Dendrites, Fingers, Cells and Free Boundary*, Springer Series in Synergetics, Springer International Publishing, 2nd edition, 2017.

[23] G. Agez, M. G. Clerc, E. Louvergneaux, and R. G. Rojas, "Bifurcations of emerging patterns in the presence of additive noise," *Physical Review E: Statistical, Nonlinear, and Soft Matter Physics*, vol. 87, no. 4, Article ID 042919, 2013.

[24] I. Steinbach, "Effect of interface anisotropy on spacing selection in constrained dendrite growth," *Acta Materialia*, vol. 56, no. 18, pp. 4965–4971, 2008.

[25] S. Gurevich, M. Amoorezaei, and N. Provatas, "Phase-field study of spacing evolution during transient growth," *Physical Review E: Statistical, Nonlinear, and Soft Matter Physics*, vol. 82, no. 5, Article ID 051606, 2010.

[26] M. Amoorezaei, S. Gurevich, and N. Provatas, "Spacing characterization in Al-Cu alloys directionally solidified under transient growth conditions," *Acta Materialia*, vol. 58, no. 18, pp. 6115–6124, 2010.

[27] W. Losert, B. Q. Shi, and H. Z. Cummins, "Evolution of dendritic patterns during alloy solidification: onset of the initial instability," *Proceedings of the National Acadamy of Sciences of the United States of America*, vol. 95, no. 2, pp. 431–438, 1998.